Talanta 103 (2013) 75–80

Contents lists available at SciVerse ScienceDirect

Talanta

journal homepage: www.elsevier.com/locate/talanta

Electrochemical immunosensor with graphene/gold nanoparticles platform and ferrocene derivatives label

Guangfeng Wang [a,b,*], Xu Gang [a,b], Xuan Zhou [a], Ge Zhang [a,b], Hao Huang [a,b], Xiaojun Zhang [a], Lun Wang [a,b,*]

[a] College of Chemistry and Materials Science, Anhui Key Laboratory of Functional Molecular Solids, Anhui Key Laboratory of Chem-Biosensing, Anhui Normal University, Wuhu 241000, PR China

[b] Anhui Key Laboratory of Controllable Chemistry Reaction & Material Chemical Engineering, Hefei University of Technology, Hefei 230009, PR China

ARTICLE INFO

Article history:
Received 4 July 2012
Received in revised form
25 September 2012
Accepted 5 October 2012
Available online 12 October 2012

Keywords:
Electrochemical immunosensor
Graphene
Ferrocene derivatives
Human IgG

ABSTRACT

In the present work, sensitive and stable sandwiched electrochemical immunosensing strategies with graphene (Gr)/gold nanoparticles (GNP) composite as the immobilization platform and ferrocene (Fc) derivatives as labels were proposed. Under the optimal choice and the proposed immunosensing strategy, with 1,1′-ferrocenedicarboxylic acid label, the human IgG could be detected specifically with a low detection limit of 0.4 ng/mL and a wide linear dynamic range from 1 to 300 ng/mL. Meanwhile, the electrochemical behavior of three different ferrocene derivatives labels was studied.

1. Introduction

Immunoassays, the determination of antibody or antigen based on biospecific recognition interactions, have been widely studied for clinical diagnosis, environmental and food analysis [1]. Various immunoassay protocols, such as surface plasmon resonance (SPR), quartz crystal microbalance (QCM), chemiluminescence's and electrochemical methods, have been extensively developed for the detection of biomarkers [2–6]. Among these methods, electrochemical immunosensors, with high sensitivity, low-cost, low power requirement, are of great value for monitoring antibody or antigen [7–10]. In the development of electrochemical immunosensing strategies, an effective immobilized biocomponents platform and a label of the immunoconjugates for signal are needed [11]. For these purposes various novel materials were prepared. Recently, Merkoci et al. reported a novel double-codified nanolabel gold nanoparticles (GNP) consisting of GNP conjugated to a horseradish peroxidase (HRP)-labeled anti-human IgG antibody for the determination of IgG by either a spectrophotometric or an electrochemical method [8]. Cui et al. [9] used horseradish peroxidase-functionalized GNP label for amplified immunoanalysis of IgG based on GNP/carbon nanotubes hybrids modified biosensor. Wang et al. [12] used ZnO/chitosan composite as immunosensor matrix for the determination of human IgG. And our group has recently fabricated IgG electrochemical immunosensor based on GNP self-assembled on L-cysteine/graphene composite platform [13].

Graphene (Gr) has emerged as an interesting material because of its unusual electronic properties and large accessible surface area [14,15]. Biocompatible Gr as a sensor platform not only presents an abundant domain for bimolecular binding but also plays a role of fast electron-transfer kinetics and further signal amplification in electrochemical detection [16,17]. For example, chitosan functionalized graphene sheets with increasing surface area were used as the biosensor platform to capture a large amount of primary antibodies [18]. Meanwhile, because of easy preparation and good biocompatibility, gold nanoparticles (GNP) have been extensively employed as immobilization platform [19–22]. The combination of Gr with GNP as a platform will be fascinating and desirable.

As we know, ferrocene (Fc) based redox active species have received much attention due to their various desirable properties [23]. And the preparation of Fc derivatives-labeled antibody is more controllable and easier than some enzyme functionalized nanomaterials label. Recently, ferrocenemonocarboyxylic acid ($Fc_{(1)}$) directly as the immunospecies marker has been studied

* Corresponding authors at: College of Chemistry and Materials Science, Anhui Key Laboratory of Functional Molecular Solids, Anhui Key Laboratory of Chem-Biosensing, Anhui Normal University, Wuhu 241000, PR China.
E-mail addresses: wangyuz@mail.ahnu.edu.cn (G. Wang), Wanglun@mail.ahnu.edu.cn (L. Wang).

0039-9140/$ - see front matter © 2012 Elsevier B.V. All rights reserved.
http://dx.doi.org/10.1016/j.talanta.2012.10.008

with satisfying result [24]. However, until now very few reports focused on the choice of other novel better Fc derivative label and the effect of Fc's group to the signal has not been discussed.

In the present work, a sensitive and stable electrochemical immunosensing strategy for the highly sensitive detection of immunospecies was proposed. The sandwiched immunosensor was constructed based on the gold nanoparticles/graphene (GNP/Gr) platform and Fc derivatives labels. And in the current work, 1,1′-ferrocenedicarboxylic acid was introduced as the probe. With 1,1′-ferrocenedicarboxylic acid ($Fc_{(3)}$) labeled antibody and the GNP/Gr platform, the human IgG could be detected specifically with a low detection limit of 0.4 ng/mL and a wide linear dynamic range from 1 to 300 ng/mL, indicating a high sensitivity. And under the same conditions, we further studied the electrochemical behavior of three different ferrocene derivatives labels with cyclic voltammetry (CV) and discussed the effect of group and structure of Fc derivatives on electrochemical character in immunosensor label. The study of group effect may improve the development and application of ferrocene derivatives in immunoassay.

2. Experimental

2.1. Reagents and apparatus

Gold (III) chloride trihydrate (99.9%), graphite and hydrazine were purchased from Shanghai Chemical Reagent Co., Ltd. Bovine serum albumin (BSA, 96–99%), human IgG (hIgG, Ag), rabbit anti-human IgG (Ab_1), goat-anti-human IgG (Ab_2) 1-(3-(dimethylamino)-propyl)-3-ethylcarbodiimidehydrochloride (EDC) and Nhydroxysulfosuccinimide (NHSS) were purchased from Biodee Biotechnology Co., Ltd (Beijing, China). Ferrocenemonocarboxylic acid ($Fc_{(1)}$), Ferrocene, $POCl_3$, other reagents and solvents were obtained from commercial suppliers and used without further purification. β-ferrocenyl-propenoicacid ($Fc_{(2)}$,) and 1,1′-ferrocenedicarboxylic acid ($Fc_{(3)}$′ were purchased from Sigma. Phosphate-buffered saline (PBS), 50 mM, with various pH values was prepared by mixing the stock solutions of NaH_2PO_4 and Na_2HPO_4 and then adjusting the pH with 0.1 M NaOH and H_3PO_4. Doubly distilled water was used throughout the experiments.

2.2. Apparatus

Scanning electron microscopy (SEM) images of the electrode surface were obtained using Hitachi S-4800 SEM (operated at 10 kV). Centrifugation was performed using a HERMLEZ 36 HK apparatus (Wehingen, Germany). Electrochemical measurements were performed on a model CHI660B electrochemical analyzer (ChenHua Instruments Co. Ltd., Shanghai, China) controlled by a personal computer. A conventional three-electrode system, consisting of a modified glassy carbon electrode (GCE) working electrode, a saturated calomel reference electrode, and a platinum wire auxiliary electrode, was employed.

2.3. Preparation of GNP/Gr modified GCE

Graphite oxide was synthesized from graphite by a modified Hummers method [25]. Polyvinylpyrrolidone (PVP)-protected Gr was prepared according to the literature [26]. Briefly, the as-purified graphite oxide suspensions were dispersed in water to create 0.05 wt% dispersion by ultrasonication for 30 min. The obtained brown dispersion was then subjected to 30 min of centrifugation at 3000 rpm to remove the unexfoliated graphite oxide (usually present in a very small amount). The homogeneous graphite oxide dispersion (5.0 mL) was mixed with 5.0 mL of 4 mg/mL PVP aqueous solution, and the mixed solution was then stirred at 50 °C for 12 h. After cooled to room temperature, to the resulting dispersion was added 20.0 μL of hydrazine solution (50 wt%) solution and 20.0 μL of ammonia solution (25 wt%). After being vigorously shaken or stirred for a few minutes, the vial was put in an oil bath (95 °C) for 1 h. The stable black dispersion was obtained. The dispersion was filtered with a nylon membrane (0.22 μm) to obtain PVP-protected graphene that can be redispersed readily in water by ultrasonication.

And then 2 μL of 1 mg/mL Gr solution after ultrasonication to form a homogeneous dispersion was dropped onto the electrochemical cleaned glassy carbon electrode (GCE) allowed to dry in ambient air for 24 h and rinsed with distilled water to get the Gr/GCE. Then, the Gr/GCE was immersed in 0.1 M KNO_3 solution containing 0.2 g/L $HAuCl_4$, conducted for 60 s at −0.26 V (vs. SCE) for the electrochemical deposition of GNP. After that the GNP/Gr/GCE was obtained.

2.4. Preparation of Fc derivatives-labeled antibody and immunoreactions procedure

The preparation of Fc derivatives-labeled antibody conjugates was carried out according to the literature [24]. Firstly, Fc derivatives of compound $Fc_{(1),\ (2)\ or\ (3)}$ (1 mg) was added to 1 mL of EDC/NHS activation aqueous solution (0.1 M each) under stirring for 2 h to activate the COOH group of the compound. Secondly, 200 μL Ab_2 (10 mg/mL) was added into the mixture, reacting for 12 h. And then the unreacted ferrocene derivative was removed via dialysis. At last, the remained $Fc_{(1),\ (2)\ or\ (3)}$–Ab_2 was brought to be stored in the refrigerator at 4 °C until use.

10 μL of 200 μg/mL Ab_1 solution was spread onto the GCE surface. After incubation for at least 2 h, they were rinsed with PBS solution containing 0.05% Tween (PBST) to remove physically absorbed Ab_1. The nonspecific binding sites of the electrodes were then blocked with the 5% BSA PBST solution for 1 h and washed with PBST. After aspiration, Ab_1 modified electrodes (Ab_1/GNP/Gr/GCE) incubated with 20 μL of detecting Ag samples with a specific concentration for 200 min. Finally, with the binding reaction between Ab_1 and Ag, the electrodes named Ag/Ab_1/GNP/Gr/GCE immersed into the 20 μL $Fc_{(1),\ (2)\ or\ (3)}$–Ab_2 solution for an incubation of 60 min to get $Fc_{(1),\ (2)\ or\ (3)}$–Ab_2/Ag/Ab_1/GNP/Gr/GCE. Following the specific interaction, the subsequent quantification of hIgG was realized by electrochemical measurement of the resulting electrode. Each incubation procedure was performed at 25 °C in order to maintain the immobilization and immunoreaction under the same experimental condition. The procedure of the sandwiched immunoreaction and the immunoassay were shown in Scheme 1.

2.5. Electrochemical measurements

All electrochemical measurements were performed using a CHI660B electrochemical workstation in a conventional three-electrode system with GCE or modified by different layers as working electrodes, a saturated calomel electrode (SCE) as reference electrode and a platinum foil electrode as counter electrode. All potentials reported were versus the SCE and all experiments were carried out at room temperature. Electrochemical alternating current impedance spectroscopy (EIS) behavior was obtained in the frequency range from 1 to 100,000 Hz with the amplitude of the applied sine wave potential 5 mV, and the formal potential of the system 0.18 V. Alternating current impedance and cyclic voltammetry (CV) characterization was carried out in 0.1 M KCl and 5 mM $K_3[Fe(CN)_6]/K_4[Fe(CN)_6]$ as a redox probe. CV and differential pulse voltammetry (DPV) of immunoassay were performed in 5 mL of 0.1 M $LiClO_4$ solution.

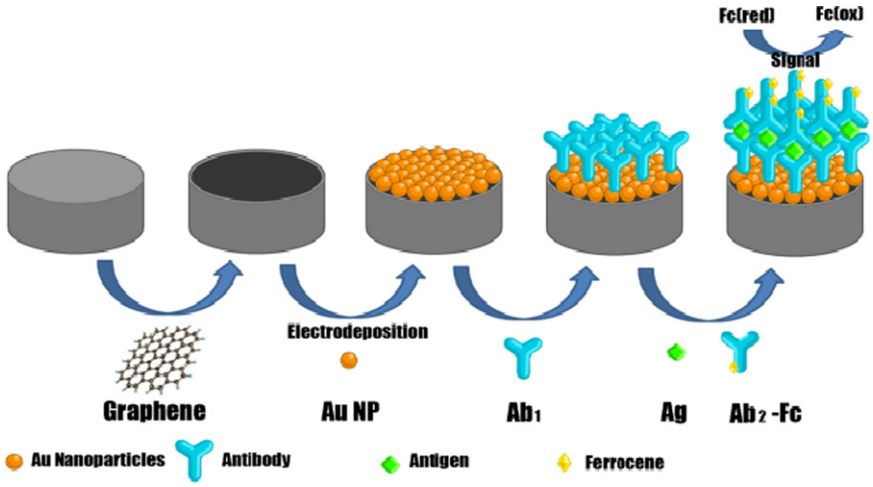

Scheme 1. Scheme of the fabrication of the immunosensor and the immunoassay procedure.

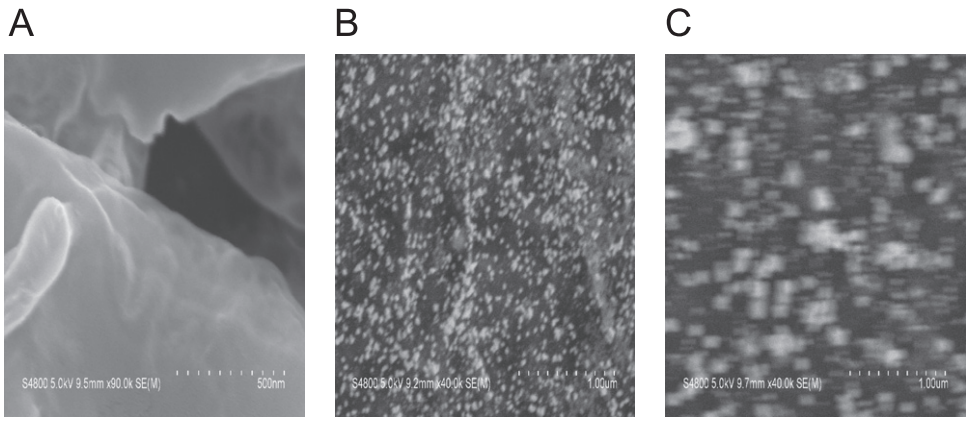

Fig. 1. Representative SEM images of Gr/GCE (A), GNP/Gr/GCE (B) and Ab_1/GNP/Gr/GCE (C).

3. Results and discussion

3.1. Characterization

3.1.1. GNP/Gr platform

Fig. 1 displays the typical SEM images of Gr (A), GNP/Gr (B), and Ab_1/GNP/Gr (C) assembled on the GCE surfaces, respectively. It is evident that individual graphene sheets were separated successfully (Fig. 1A) and these 2-D sheets served as a foundation for the electrodeposition of GNP stably as seen from Fig. 1B. Compared images B with C, the GNP/Gr became rougher. We might conclude that the Ab_1 molecules were adsorbed on the surface of the GNP/Gr by the covalent bonding of Au of GNP and $-NH_2$ of the protein, which made the conductivity worse.

3.1.2. The immunosensor

EIS would provide detailed information on change of the surface property of modified electrodes for each modification process. The typical impedance spectrum (presented in the form of the Nyquist plot) includes a semicircle portion at higher frequencies corresponding to the electron-transfer-limited process and a linear part at lower frequency range representing the diffusion-limited process [27]. The diameter of the semicircle in the impedance spectrum is equal to the electron-transfer resistance, Ret, which reflects the electron transfer kinetics of the redox probe at the electrode surface. Fig. 2 shows the impedance spectra corresponding to the stepwise modification processes. Curves a and b impedance spectroscopy are of the bare GCE and GNP/Gr modified GCE. GNP/Gr modified GCE exhibits an almost straight line in the Nyquist plot of impedance spectroscopy, characteristics of a diffusion-limited electron-transfer process, indicating that GNP/Gr film acts as high electron relay for shuttling electron between the electrochemical probe and the electrode. After immobilization of Ab_1, an obvious semicircle part of the impedance spectrum appears, and the Ret increases to 7346 Ω (Fig. 2 curve c), hindering the electron-transfer of the electrochemical probe. Especially, after Ag molecules were reacted with Ab_1, a remarkable increase of interfacial resistance is obtained as 10,320 Ω on the modified electrode (Fig. 2, curve d). The reason is that the immunocomplex layer on the electrode acts as the electron communication and mass-transfer blocking layer, further insulating the conductive support and hindering the access of redox probe towards the electrode surface significantly, thus, a further increase in Ret was observed. At last when $Fc_{(1)}$–Ab_2 label coupled with Ag, surprisingly, the Ret decreased to 1658 Ω (Fig. 2, curve e). We suggest it may be due to electrostatic adsorption between $Fc_{(1)}$ and the probe. The EIS change of the modified process indicated that the protein was immobilized on the electrode surface firmly and retained high bioactivity and the immunoreaction could be completed with the method. We also study the control experiments of 1,1′-ferrocenedicarboxylic acid ($Fc_{(3)}$) oxidation on bare GCE, GCE modified with graphene or gold nanoparticles, as shown in Fig. 2B. We find that graphene or Au

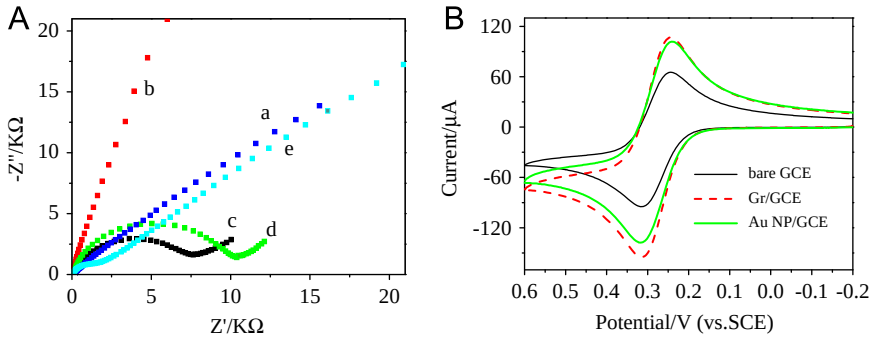

Fig. 2. (A) EIS characterization of bare GCE (a), GNP/Gr/GCE (b), Ab_1/GNP/Gr/GCE (c), Ag/Ab_1/GNP/Gr/GCE (d) and $Fc_{(1)}$-Ab_2/Ag/Ab_1/GNP/Gr/GCE (e) modified GCE in 5 mM $K_3Fe(CN)_6$ with 0.1 M KCl solution; (B) $Fc_{(3)}$ on different modified GCE in 0.1 M $LiClO_4$ at a scan rate of 100 mV/s.

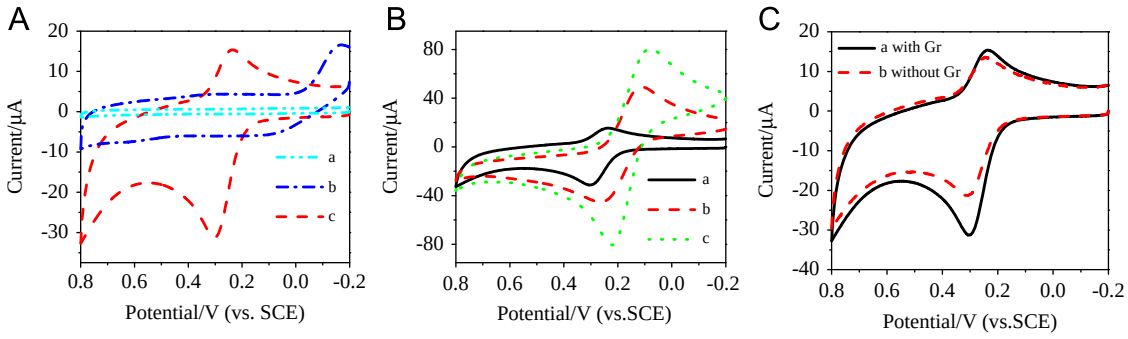

Fig. 3. CVs of (A) bare GCE (a), GNP/Gr (b), and $Fc_{(1)}$-Ab_2/Ag/Ab_1/GNP/Gr (c); (B) $Fc_{(1)}$ (a), $Fc_{(2)}$ (b) and $Fc_{(3)}$ (c)-Ab_2/Ag/Ab_1/GNP/Gr; (C) $Fc_{(1)}$-Ab_2/Ag/Ab_1/GNP/Gr (a) and $Fc_{(1)}$-Ab_2/Ag/Ab_1/Gr (b) modified GCE in 0.1 M $LiClO_4$ at a scan rate of 100 mV/s.

NP modified electrode has better electron transfer capability than bare GCE that makes current of $Fc_{(3)}$ larger.

3.2. The electrochemical character of the modified electrode

In the present immunosensor, as shown in Fig. 3A, first, as curves a and b show, on the bare and Gr/GNP modified GCE there is no redox peaks. And then the GNP/Gr platform was ready for the antibody attachment due to the Au–amine interaction. The introducing of Ab_1 and Ag also shows no redox peaks but the charge currents increase (not shown). Then after the $Fc_{(1)}$-labeled antibody reacted with the Ag, a remarkable redox peak current was observed (curve c), originated from the redox of Fc. So making use of the unique structure and electronic properties of ferrocene, the specific antigen can be sensitively detected.

The electrochemical characters of the three Fc derivatives labels were also studied. As shown in Fig. 3B, with the same amount of Ag, under the same conditions, the order of the peak currents is $Fc_{(1)} < Fc_{(2)} < Fc_{(3)}$ label, which shows $Fc_{(3)}$ label is the best label among the three. We think that it may be relative to its structure. $Fc_{(3)}$ provided a matrix with more COOH-groups for labeling; presented a high loading of antibody molecules and reserved a higher immunological activity by the structure. However, $Fc_{(2)}$ with more π electrons conjugation in structure may generate a large number of electrons during electrochemical reaction, which could serve to amplify the electrochemical signal and therefore enhance the detection sensitivity. But it seems the effect of COOH-group is more than that of the π electrons conjugation.

We also study the role of Gr in the immunosensor, as shown in Fig. 3C, the immunosensor fabricated with Gr has larger response than that without Gr, which means Gr may play a role of signal amplificaiton.

3.3. Optimization of experimental conditions

Parameters of the assay procedure, affecting the response of the immunosensor, were investigated. To find the proper immune pH, we investigated the influence of pH on the performance of the immunosensor over the pH range of 5.0–10.0 (Fig. 4A). Highly acidic or alkaline surroundings showed poor response for they would damage the immobilized protein, especially in alkalinity. An ideal pH of 7.4 was chosen for the assay experiments, which is also a general pH value in immunology.

The time-course of the IgG assembly on the hybrids was investigated by the electrochemical response signal to optimize the immobilization time (Fig. 4B). The experimental data indicated that assembly time has some effect on the response signal, which implies that the adsorption quantity of antibody relies much on the time accretion. In this work, an incubation time of 200 min could be recommended.

The effect of the concentration of rabbit anti-hIgG antibody (Ab_1) from 50 to 600 μg mL^{-1} on the immobilization efficiency was investigated (Fig. 4C). Our experimental data revealed the highest response was observed at 200 μg mL^{-1}; whereas, gradually increasing concentration leaded to a slight decrease signal. The possible reason is that only antibodies adsorbed on the hybrids with suitable orientation can participate in the immunoreaction and higher concentration might increase disorder in alignment of adsorbed antibody and steric hindrance of immunoreaction. Therefore, 200 μg mL^{-1} Ab_1 was chosen in the present experiment.

3.4. The DPV of the immunosensor

Under the optimal immunoassay conditions, the calibration plot for the detection of IgG was studied as Fig. 5 shows.

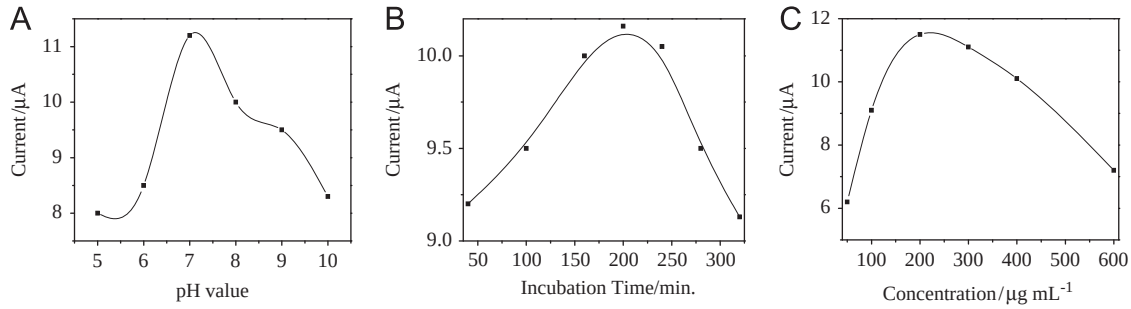

Fig. 4. Effects of (A) pH of detection solution, (B) incubation time, and (C) the amount of Ab_1 on the immunosensor.

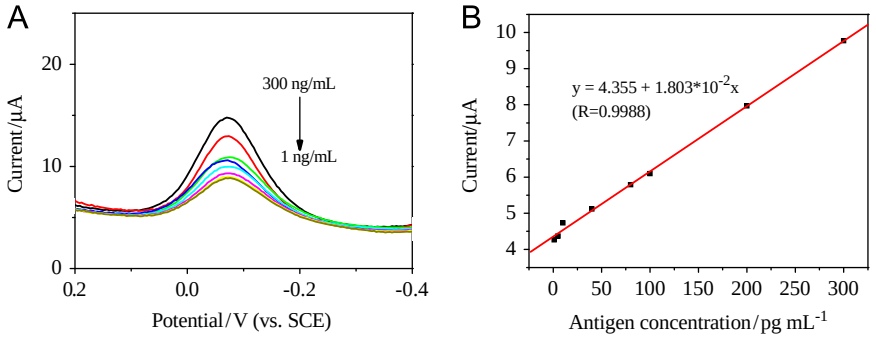

Fig. 5. Typical DPV of electrochemical immunoassay with $Fc_{(3)}$ label in 0.1 M $LiClO_4$ with increasing HIgG concentration of 1, 5, 10, 40, 80, 100, 200 and 300 ng/mL, respectively (A); the resulting calibration curve (B).

Table 1
Regression equation of electrochemical immunosensor with different labels.

Label	Linear equation	*R*
$Fc_{(1)}$	$I\ (\mu A)=1.593+6.136\times10^{-3}c\ (pg/mL)$	0.9999
$Fc_{(2)}$	$I\ (\mu A)=3.998+1.193\times10^{-2}c\ (pg/mL)$	0.9988
$Fc_{(3)}$	$I\ (\mu A)=4.355+1.803\times10^{-2}c\ (pg/mL)$	0.9969

The proposed immunosensor that was incubated with different concentrations of antigen solution in turn was examined by DPV in 5 mL 0.1 M $LiClO_4$. It was found that the peak current of DPV performed in proportion to concentrations of antigen from 1 to 300 ng/mL with different regression equation respectively. According to the figures and the equations, we also could find that $Fc_{(3)}$ label shows the highest response under the same conditions which is the same with the result in CV of Fig. 3B (Table 1). With $Fc_{(3)}$ label, the detection limit was 0.4 ng/mL based on a signal-to-noise ratio of 3 indicating a high sensitivity. Such low detection limit achieved by the present sensing system was comparable with the values reported in some literature (Table 2). Our results demonstrated that the immunosensor exhibited wider linear range and a lower detection limit.

3.5. *Selectivity, reproducibility and stability*

To monitor the selectivity of the immunosensor, various tumor markers including carcinoma antigen 125 (CA 125), carcinoembryonic antigen (CEA), and prostate-specific antigen (PSA) were used. The electrochemical signals were recorded in 100, 200, and 300 ng/mL IgG with/without interfering agent, respectively. Experimental results indicated that the current shifts were relatively obvious when using low IgG concentration and interfering agent of high concentration. The reason might be the fact that the interfering agent of high concentration was physically adsorbed on the base electrode. To overview this issue, the selectivity of the immunosensor is acceptable. Meanwhile, the reproducibility of the immunosensor was evaluated by using the coefficient of variation of intra- and inter-assays. Taking 100, 200 and 300 ng/mL IgG for examples, the intra-assay and inter-assay of the immunosensor was evaluated using one immunosensor for five repeat assays and five immunosensors for one time assay, respectively. The RSDs of the intra-assay and inter-assay were 4.2%, 6.1%, 4.9% and 5.2%, 5.9%, 6.7% for 100, 200 and 300 ng/mL IgG, respectively. Thus, the reproducibility of the immunosensor is satisfactory The stability was investigated over a 30-day period when the sensor was stored at 4 °C in pH 6.8 PBS. It was measured intermittently (every 3–5 days), no obvious change of the response was found over this period, indicating the storage stability of the immunoassay system was accepted.

The feasibility of the immunoassay system for clinical applications was investigated by analyzing several real samples. In comparison with the ELISA method, these serum samples were diluted to different concentrations with a PBS of pH 7.4. Table 3 describes the correlation between the results obtained by the proposed immunosensor and the ELISA method. As the result shows, it is feasible for detection of antigen with this immunosensor.

4. Conclusion

This reports a novel electrochemical immunosensor for the detection of IgG. The immunosensor was fabricated using a GNP/Gr platform with low-toxic, high-conductive Fc derivatives for the label of secondary antibody. With $Fc_{(3)}$ label, the detection limit of IgG was 0.4 ng/mL. The highly sensitive electrochemical immunosensors are favorable for the detection of low concentration sample. Highlight of this work is to exploit a novel platform and label for the performance improvement of the electrochemical immunosensors. The study of group effect may be useful for choice of better ferrocene derivatives labels and may

Table 2
Comparison with other electrochemical immunosensor.

Enhancement materials	Linear Range/ng ml^{-1}	Detection limit/ng ml^{-1}	Ref.
ZnO/chitosan composite	2.5–500	1.2	[28]
Gold nanoparticles	2–32	2	[29]
COOH-multiwalled carbon nanotubes/Fe_3O_4	30–1000	25	[30]
Plasma-activated multi-walled carbon nanotube-polystyrene	3–100	–	[31]
Gold nanoparticle/L-cysteine	0.5–25	0.16	[32]
Gold nanoparticle	5–500	1.1	[33]
Three-dimensional sol–gel	1.12–162	0.56	[34]
Colloidal gold-graphite-teflon	5–100	2.6	[35]
Gold nanoparticles–polyethylenimine	–	10	[36]
colloidal gold	10.9–10,900	3.5	[37]
Gold colloid monolayers associated with a sol–gel matrix	8.3–2128	3.3	[38]
Magnetic nanoparticles	600–34,900	360	[39]
Tetrathiafulvalene	5–100	–	[40]
$[Fe(CN)_6]^{3-}$	10–10,000	3	[41]
Gr/Au	1–300	0.4	Our work

Table 3
Analysis results of IgG for human serum specimen.

Samples	IgG IgG concentration by ELISA[a] (ng/mL)	IgG concentration by EIA[b] (ng/mL)
1	48.2	52.5
2	107.3	108.2
3	249.1	243.8
4	297.8	303.6
5	326.1	323.8

[a] Enzyme–linked immunosorbent assay method.
[b] Electrochemical immunosensing assay method. As the IgG concentration level of human serum is very high, the human serum specimens have to be diluted to the detection range of the electrochemical immunosensors by using PBS (pH 7.4) buffer according to the IgG concentration by ELISA.

improve the development and application of ferrocene derivatives in immunoassay.

Acknowledgment

This work was financially supported by the projects (20901003, 21073001, 21005001 and 21075002) from the National Natural Science Foundation of China, the Natural Science Foundation of Anhui (KJ2009B013Z, KJ2012A139) and the project of the Anhui Key Laboratory of Controllable Chemistry Reaction & Material Chemical Engineering (OFCC0905).

References

[1] Y.H. Liao, R. Yuan, Y.Q. Chai, Y. Zhuo, X. Yang, Anal. Biochem. 402 (2010) 47.
[2] J. Ehrhart, B. Bennetau, L. Renaud, J. Madrange, L. Thomas, J. Morisot, A. Brosseau, P. Tran, Biosens. Bioelectron. 24 (2008) 467.
[3] N. Kim, D.K. Kim, Y.J. Cho, D.K. Moon, W.Y. Kim, Biosens. Bioelectron. 24 (2008) 391.
[4] M. Wasowicz, S. Viswanathan, A. Dvornyk, K. Grzelak, B. Kludkiewicz, H. Radecka, Biosens. Bioelectron. 24 (2008) 191.
[5] Z.J. Yang, Z.F. Fu, F. Yan, H. Liu, H.X. Ju, Biosens. Bioelectron. 24 (2008) 35.
[6] R. Niessner, D. Knopp, Biosens. Bioelectron. 24 (2009) 2125.
[7] D.P. Tang, R. Yuan, Y.Q. Chai, Anal. Chim. Acta 2 (2006) 158.
[8] A. Ambrosi, M.T. Castaneda, A.J. Killard, M.R. Smyth, S. Alegret, A. Merkoci, Anal. Chem. 79 (2007) 5232.
[9] R.J. Cui, H.P. Huang, Z.Z. Yin, D. Gao, J.J. Zhu, Biosens. Bioelectron. 23 (2008) 1666.
[10] K. Shang, J. Zhu, X. Meng, Z. Cheng, S. Ai, Biosens. Boelectron. 37 (2012) 107.
[11] J. Chen, J.H. Tang, F. Yan, H.X. Ju, Biomaterials 271 (2006) 2313.
[12] Z.J. Wang, Y.H. Yang, J.S. Li, J.L. Gong, G.L. Shen, R.Q. Yu, Talanta 69 (2006) 686.
[13] G.F. Wang, H. Huang, G. Zhang, X.J. Zhang, B. Fang, L. Wang, Anal. Method 2 (2010) 1692.
[14] A.K. Geim, K.S. Novoselov, Nat. Mater. 6 (2007) 183.
[15] L.H. Tang, Y. Wang, Y.M. Li, H.B. Feng, J. Lu, J.H. Li, Adv. Funct. Mater. 19 (2009) 1.
[16] Y.M. Li, L.H. Tang, J.H. Li, Electrochem. Commun. 11 (2009) 846.
[17] X.H. Kang, J. Wang, X.H. Kang, H. Wu, I.A. Aksay, J. Liu, Y.H. Lin, Biosens. Bioelectron. 25 (2009) 901.
[18] D. Du, Z.X. Zou, Y.S. Shin, J. Wang, H. Wu, H.Engelhard. Mark, J. Liu, A.Aksay. Ilhan, Y.H. Lin, Anal. Chem. 82 (2010) 2989.
[19] M.C. Daniel, D. Astruc, Chem. Rev. 104 (2004) 293.
[20] Y.C. Yang, S.W. Dong, T. Shen, C.X. Jian, H.J. Chang, Y. Li, J.X. Zhou, Electrochim. Acta 56 (2011) 6021.
[21] B. Liu, D. Tang, J. Tang, B. Su, Q. Li, G. Chen, Analyst 136 (2011) 2218.
[22] S.P. Wang, Z.S. Wu, F.L. Qu, S.B. Zhang, G.L. Shen, R.Q. Yu, Biosens. Bioelectron. 4 (2008) 1026.
[23] F.O. Laforge, T. Kakiuchi, F. Shigematsu, M.V. Mirkin, J. Am. Chem. Soc. 126 (2004) 15380.
[24] S.B. Zhang, F. Zheng, Z.S. Wu, G.L. Shen, R.Q. Yu, Biosens. Bioelectron. 24 (2008) 129.
[25] W. Hummers, R. Offeman, J. Am. Chem. Soc. 80 (1958) 1339.
[26] C.S. Shan, H.F. Yang, J.F. Song, D.X. Han, A. Ivaska, L. Niu, Anal. Chem. 81 (2009) 2378.
[27] A.J. Bard, L.R. Faulkner. Electrochem. Methods, 1980.
[28] Z.J. Wang, Y.H. Yang, J.S. Li, J.L. Gong, G.L. Shen, R.Q. Yu, Talanta 69 (2006) 686.
[29] G.K. Ahirwal, C.K. Mitra, Biosens. Bioelectron. 25 (2010) 2016.
[30] H. Zarei, H. Ghourchian, K. Eskandari, M. Zeinali, Anal. Biochem. 421 (2012) 446.
[31] C. Fernández-Sánchez, E. Pellicer, J. Orozco, C. Jiménez-Jorquera, L.M. Lechuga, E. Mendoza, Nanotechnology 20 (2009) 335501.
[32] L.Y. Zhang, Y. Liu, T. Chen, Microchim. Acta 164 (2009) 161.
[33] C. Leng, G.S. Lai, F. Yan, H.X. Ju, Anal. Chim. Acta 97 (2010) 97.
[34] S.B. Wang, D.Y. Tang, Bioprocess. Biosyst. Eng. 31 (2008) 385.
[35] V. Carralero, A. González-Cortés, P. Yá ˜nez-Sede ˜no, J.M. Pingarrón, Anal. Lett. 41 (2008) 244.
[36] H.Q. Li, C.G. Wang, Z.F. Ma, Z.M. Su, Anal. Bioanalytic. Chem. 384 (2008) 1518.
[37] R. Slavik, J. Homola, J. Ctyrok, E. Brynda, Sensors Actuat. B 114 (2006) 696.
[38] Z.W. Tang, K.M. Wang, W.H. Tan, C.B. Mao, et al., Anal. Chim. Acta 528 (2005) 235.
[39] K. Taniwaki, A. Hyakutake, T. Aoki, M. Yoshikawa, M. Guiver, Anal. Chim. Acta 481 (2003) 191.
[40] F. Wendzinski, B. Gründig, R. Renneberg, F. Spener, Biosens Bioelectron. 12 (1997) 43.
[41] L.P. Qiu, C.C. Wang, P. Hu, Z.S. Wu, G.L. Shen, R.Q. Yu., Talanta 83 (2010) 42.